Respiratory Motion Estimation using a 3D Diaphragm Model

Marco Bögel[1,2], Christian Riess[1,2], Andreas Maier[1], Joachim Hornegger[1], Rebecca Fahrig[2]

[1]Pattern Recognition Lab, FAU Erlangen-Nürnberg
[2]Department of Radiology, Lucas MRS Center, Stanford University, Palo Alto, CA, USA
marco.boegel@informatik.stud.uni-erlangen.de

Abstract. Long acquisition times of several seconds lead to image artifacts in cardiac C-arm CT. These artifacts are mostly caused by respiratory motion. In order to improve image quality, it is important to accurately estimate the breathing motion that occurred during image acquisition. It has been shown that diaphragm motion is correlated to the respiration-induced motion of the heart. We present a method to estimate an accurate three-dimensional (3D) model of the diaphragm and its compression motion field from a set of C-arm CT projection images acquired during free breathing. First results on the digital XCAT phantom are promising. The method is able to estimate the motion field amplitude exactly. The boundaries of the estimated compression motion field are estimated within 3 mm accuracy.

1 Introduction

C-arm CT enables reconstruction of 3D images during medical procedures. However, long acquisition times of several seconds, during which the heart is beating and the patient might breathe, may lead to image artifacts, such as motion blurring or streaks. A widely used technique to reduce breathing motion is the single breath-hold scan. The physician instructs the patient to hold his breath after expiration. Projection images are acquired during a single breath-hold. Although this approach is widely used, multiple studies have shown that breath-holding does not eliminate breathing motion entirely and there is significant residual motion. Monitoring the position of the right hemidiaphragm during breath-hold, Jahnke et al. observed residual breathing motion to a certain extent for almost half their test group [1]. Therefore, it is necessary to develop methods to estimate and compensate for respiratory motion in cardiac C-arm CT.

There are many ways to estimate respiratory signals. Many are based on additional hardware, e.g. Time of Flight- or stereo vision-cameras. Other techniques aim to extract the respiratory signal directly from the projection images. Image-based respiratory motion extraction often relies on tracking of fiducial markers in the projection images [2,3]. Wang et al. have shown that the motion of the diaphragm is highly correlated to respiration-induced motion of the heart [4].

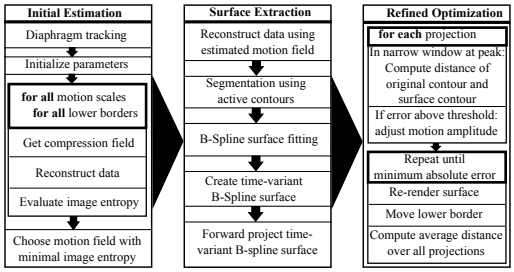

Fig. 1. Diagram of the proposed algorithm.

Sonke et al. propose to extract a one-dimensional breathing signal by projecting diaphragm-like features on the cranio-caudal axis and to select the features with the largest temporal change [5]. Similar techniques using diaphragm tracking in projection images have been proposed recently [6,7]. Motion estimation approaches based on the diaphragm motion are limited as they only take into account the motion at the diaphragm top. With the presented approach we aim to use the whole diaphragm surface to measure respiratory motion.

2 Materials and Methods

We propose a method to estimate diaphragm motion as a compression motion field in two optimization steps. First we do an initial estimation which will yield a reconstruction with reasonably good diaphragm-lung contrast, which is then used to segment the diaphragm. The acquired diaphragm model is utilized in the second step to register the model to the projection images. For reconstruction we use a voxel-driven motion-compensated reconstruction algorithm by Schäfer et al. [8]. A flow diagram of the proposed method is provided in Figure 1.

2.1 Initial Estimation

In this method we assume that respiratory diaphragm motion can be modelled as a compression motion field. During inspiration the diaphragm is compressed, however respiratory motion is limited by a fixed lower plane where no motion occurs. Therefore, to lower parts of the diaphragm surface less motion is applied than to the diaphragm top. The top of the diaphragm at expiration state defines an upper border for the compression field.

In order to estimate a compression motion field, we need to estimate a lower and upper border of the motion field, as well as the motion amplitude that is measured at the upper border. We use a diaphragm-tracking algorithm from previous work [7] to acquire some prior information. We can get the 3D position of the diaphragm top for each projection by triangulation of the diaphragm vertices, as well as a 1D motion signal using only the z-coordinates of the triangulated points. Additionally we also get a segmentation of the diaphragm in 2D projection space.

Afterwards, the 1D motion field that was acquired through diaphragm tracking is processed to determine the indices of inspiration and expiration. Then, the signal is normalized to a maximum range of $[-1.0, 1.0]$. Additionally, we choose the upper border of the compression field as the triangulated 3D world coordinate position of the diaphragm during expiration. To account for triangulation errors we choose the upper plane slightly above the triangulated point.

Optimizing the motion field requires a large number of reconstructions using different motion fields. In order to reduce computation time we choose to reconstruct very small volumes of 128^3 voxels, with a resolution of $2.0\frac{\text{mm}}{\text{voxel}}$. As we show in this work, this is sufficient to evaluate the diaphragm and lung contrast using image entropy.

Using prior knowledge we reduce the search space for the optimal scale to a small window of 10 mm around the absolute maximum magnitude of the triangulated signal. The search space for lower borders can be narrowed down based on the visibility of the diaphragm in the projections. We chose a relatively large step size of approximately 10% of the volume size for the lower border.

In order to assess the image quality we chose an ROI centered around the diaphragm top. We measure how badly the diaphragm-lung interface is blurred using the image entropy. We choose a relatively narrow ROI of 4 cm diameter. The height of the ROI spans the lower half of the volume. For the proposed 128^3 voxel volume with $2.0\frac{\text{mm}}{\text{voxel}}$ resolution, this results in an ROI of $40 \times 40 \times 128$ mm. The center of this ROI is the triangulated top of the diaphragm at expiration state. Shannon entropy is a measure of uncertainty, and is denoted by

$$H(X) = -\sum_{i=1}^{N} p(x_i) \cdot \ln(p(x_i)). \tag{1}$$

In order to get the probabilities $p(x_i)$ for each intensity value x_i, a histogram over the intensities in the ROI is computed. In our implementation we chose to use 100 bins. Figure 2 shows two histograms corresponding to an uncompensated and a compensated reconstruction. The first histogram in Figure 2(a) shows one large peak at low intensities corresponding to the lungs. However, many intensities are similarly frequent, which means relatively high uncertainty. In comparison, the histogram of the correct reconstruction in Figure 2(b) shows only two large peaks at intensities corresponding to lungs and diaphragm. Thus, there is very low uncertainty in the image.

We use the compression field that results in the best image entropy to reconstruct the set of projection images of the 2D segmented diaphragm. Based on this reconstruction we can segment the diaphragm using an active contour segmentation, which results in a 3D surface mesh of the diaphragm.

In order to get a smooth surface and reduce segmentation inaccuracies, we approximate the mesh as a uniform cubic surface B-spline. This B-spline representation allows us to use very efficient projection algorithms to speed up the registration process in the next step.

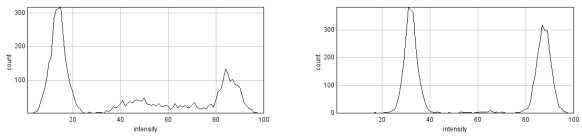

(a) uncompensated (b) compensated

Fig. 2. Histograms of the intensities in the ROI around the diaphragm top of an uncompensated reconstruction and an optimized one.

2.2 Refined Optimization

While the initial motion field estimation provided relatively good results, we limited our approach to very small reconstruction volumes in order to reduce computational effort. Our estimation algorithm was able to find a good approximation of the motion field, however, close to the correct motion field, the results of our image entropy measurements are very similar, which is in part caused by the smoothing effect of our small volumes and the relatively large step size we used in the estimation of the lower compression field border. With the following method we aim to refine our estimated compression motion field, using a registration approach.

First, we create a time variant surface B-spline by adding the compression motion field to the B-spline control points. In order to get a good time-resolution a surface B-spline is created in this way for each projection. Afterwards, we want to compute forward projections of this time-variant surface B-spline, using the GPU [9]. With this approach we are able to create one forward projection of our B-spline in approximately $20 - 40$ ms.

Our aim is to register the forward projection of the diaphragm B-spline model to the original projection images that include the respiratory motion, using a very quick contour-based approach. Due to the fact that our new forward projections only contain the diaphragm, contour detection is trivial. With the contours available, we separately estimate the motion magnitude and the lower border of the compression field.

Estimation of Motion Amplitude First, we adjust the motion amplitude, so that the tops of the two contours are aligned. In order to determine how to adjust the magnitude, we measure the average distance of the two contours in a narrow window of 40 pixels around the top. If the average distance exceeds a predefined threshold, we adjust the motion field magnitude for this surface B-spline. For the XCAT phantom we chose a threshold of 1 pixel. We can adjust the amplitude either iteratively with a predefined step size, or we can re-project the top points of both contours onto the plane that passes through the 3D diaphragm top of the initial diaphragm tracking and that is parallel to the detector. We can then update the motion field magnitude using the difference of the 3D spline top position and the 3D position of the tracked diaphragm.

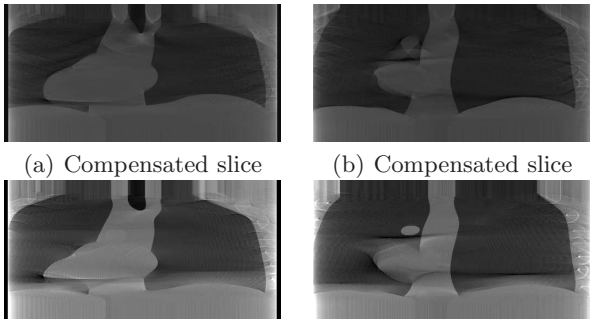

(a) Compensated slice (b) Compensated slice

(c) Uncompensated slice corresp. to (a) (d) Uncompensated slice corresp. to (b)

Fig. 3. Comparison of image quality of two coronary slices of an uncompensated reconstruction of the XCAT phantom and an optimized one.

Estimation of Compression Border After updating the motion field magnitude, the updated time-variant surface B-spline is forward projected again. The peaks of the original and spline contours are now aligned. Now, the slope of the B-spline contour is either too steep or too flat. This can be adjusted by lifting or lowering the lower border of the compression field. We can determine in which direction the lower border has to be moved by looking at the average error distance over all projection images. The lower border is moved by an arbitrary step size in each iteration, until the average error is below a predefined threshold.

3 Results

We evaluated our estimated motion fields on the digital XCAT phantom using projections of a breathing thorax. An acquisition protocol of four seconds with a full respiration cycle with 24 mm diaphragm amplitude was simulated to create 200 projection images of size 640×480 pixels with a resolution of $0.616\,\frac{\text{mm}}{\text{pixel}}$. The compression motion field used in the phantom had the lower boundary placed at -98 mm and the upper diaphragm boundary at -38 mm.

We evaluated the initial estimation on lower boundaries ranging from -179 mm to -75 mm, with a step size of 26 mm. The correct minimum for the motion amplitude was found at 24 mm. We also observed similarly low image entropy at scales close to 24 mm even for incorrect lower borders. The optimal border detected by the initial estimator is located at -101 mm. Using smaller steps of 2 mm, we are not able to further increase the accuracy.

Refining the motion field in this case yields only slight changes at individual projections. Figure 3 shows reconstruction results for two coronary slices through the two hemidiaphragms. Image contrast at the diaphragm is considerably improved as we observe very clear diaphragm contours, even at the sides.

4 Discussion

As results on the XCAT phantom show, our method allows us to estimate a compression motion field of the diaphragm based on free-breathing C-arm CT projection data. We are able to estimate the amplitude of the diaphragm motion as well as the lower boundary of the compression field. Studies have shown that the motion of the diaphragm is highly correlated to respiration-induced motion of the heart [4]. An accurate motion signal of the diaphragm can be used as a surrogate signal to drive an elastic respiratory motion model of the heart.

The presented method works well with reconstructions of low resolution in order to reduce computational effort. Our initial optimization-based on image entropy works very well, and might possibly be accurate enough in many cases without further refinement, as it is able to estimate the motion amplitude accurately, and the compression boundaries within 3 mm accuracy.

Future work will deal with the interpolation of the diaphragm motion vector field with a respiratory heart motion model, in order to compensate residual breathing motion in breath-hold scans.

References

1. Jahnke C, Paetsch I, Achenbach S, Schnackenburg B, Gebker R, Fleck E, et al. Coronary MR Imaging: Breath-hold Capability and Patterns, Coronary Artery Rest Periods, and beta-Blocker Use. Radiology. 2006;239:71–78.
2. Wiesner S, Yaniv Z. Respiratory Signal Generation for Retrospective Gating of Cone-Beam CT Images. Proc SPIE. 2008;6918:691817–1 – 691817–12.
3. Marchant TE, Price GJ, Matuszewiski BJ, Moore CJ. Reduction of motion artefacts in on-board cone beam CT by warping of projection images. Br J Radiol. 2011 March;84:251–264.
4. Wang Y, Riederer S, Ehman R. Respiratory motion of the heart: Kinematics and the implications for spatial resolution in coronary imaging. Magn Reson Med. 1995;33:716–719.
5. Sonke JJ, Zijp L, Remeijer P, van Herk M. Respiratory correlated cone beam CT. Med Phys. 2005;32:1176–1186.
6. Chen M, Siochi RA. Diaphragm motion quantification in megavoltage cone-beam CT projection images. Med Phys. 2010;37(5):2312–2320.
7. Bögel M, Hofmann HG, Hornegger J, Fahrig R, Britzen S, Maier A. Respiratory Motion Compensation Using Diaphragm Tracking for Cone-Beam C-Arm CT: A Simulation and a Phantom Study. International Journal of Biomedical Imaging. 2013;2013:1–10.
8. Schäfer D, Jandt U, Carroll JD, Grass M. Motion compensated reconstruction for rotational X-ray angiography using 4D coronary centerline models. In: Proc Fully 3D; 2007. p. 245–248.
9. Maier A, Hofmann H, Schwemmer C, Hornegger J, Keil A, Fahrig R. Fast Simulation of X-ray Projections of Spline-based Surfaces using an Append Buffer. Phys Med Biol. 2012;57(19):6193–6210.